

Published in final edited form as:

Curr Opin Neurobiol. 2011 April ; 21(2): 313–321. doi:10.1016/j.conb.2011.02.008.

The mechanisms underlying the spatial spreading of signaling activity

Ryohei Yasuda^{1,2} and Hideji Murakoshi¹

¹Department of Neurobiology, Duke University Medical Center

²Howard Hughes Medical Institute

Abstract

During the induction of plasticity of dendritic spines, many intracellular signaling pathways are spatially and temporally regulated to coordinate downstream cellular processes in different dendritic micron-domains. Recent advent of imaging technology based on fluorescence resonance energy transfer (FRET) has allowed the direct monitoring of the spatiotemporal regulation of signaling activity in spines and dendrites during synaptic plasticity. In particular, the activity of three small GTPase proteins HRas, Cdc42 and RhoA, which share similar structure and mobility on the plasma membrane, displayed different spatial spreading patterns: Cdc42 is compartmentalized in the stimulated spines while RhoA and HRas spreads into dendrites over 5–10 μm . These measurements thus provide the basis for understanding the mechanisms underlying the spatiotemporal regulation of signaling activity. Further, using spatiotemporally controlled spine stimulations, some of the roles of signal spreading have been revealed.

Introduction

Postsynaptic signaling is important for many forms of neuronal plasticity including long-term potentiation (LTP) and depression (LTD), which are believed to be the cellular basis of learning and memory. In neurons, the signaling dynamics can be physically restricted in subcellular compartments with wide-ranging length scales, from dendritic or axonal branches ($> \sim 10 \mu\text{m}$) to synaptic compartments such as dendritic spines and axonal boutons ($\sim 1 \mu\text{m}$) to nanometer scale signaling complexes near channels and receptors [1]. The compartmentalization of signaling shapes its spatiotemporal dynamics. In particular, dendritic spines, the postsynaptic compartments where most excitatory synapses reside, present a unique environment containing channels, receptors, scaffolding proteins and enzymes in an extremely small volume (~ 0.1 femtoliters) [2]. Signaling activity in each spine is compartmentalized due to its narrow neck (~ 100 nm in diameter) connecting the spine head and dendrite and, to some extent, regulated independently from neighboring spines [3,4]. Due to this signal compartmentalization, LTP and associated spine enlargement can be induced in single dendritic spines without affecting surrounding spines [5]. However, it has been reported that the length scale of some forms of dendritic plasticity can be larger than a single spine and involve multiple spines [6, 7*, 8]. Recently, the activity of several signaling proteins in single spines during LTP and associated spine structural plasticity has

© 2011 Elsevier Ltd. All rights reserved.

Corresponding author: Yasuda, Ryohei (yasuda@neuro.duke.edu).

Publisher's Disclaimer: This is a PDF file of an unedited manuscript that has been accepted for publication. As a service to our customers we are providing this early version of the manuscript. The manuscript will undergo copyediting, typesetting, and review of the resulting proof before it is published in its final citable form. Please note that during the production process errors may be discovered which could affect the content, and all legal disclaimers that apply to the journal pertain.

been imaged, and this revealed complicated spatiotemporal integration of postsynaptic signal transduction during LTP [9, 10*, 11*].

Spatiotemporal dynamics of signaling in single spines

FRET imaging with 2-photon fluorescence lifetime imaging

The spatiotemporal dynamics of intracellular signaling have been imaged optically using fluorescence resonance energy transfer (FRET) in combination with FRET-based signaling sensors [12]. FRET is the photo-physical process that occurs between two fluorophores in which the energy of an excited donor fluorophore is transferred to an acceptor fluorophore. FRET efficiency decays rapidly as the distance between two fluorophores increases, and become essentially zero at ~10 nm [13]. Thus, FRET can be used as a readout of the interaction between proteins tagged with fluorophores and the conformational change of a protein tagged with two fluorophores [14]. A number of FRET sensors which can sense signaling events, including changes in second messenger concentration and activity of enzymes, have been developed [12]. These techniques, however, have been difficult to implement for imaging spine signaling due to the small fluorescence from the tiny volume of spines and strong light scattering by brain tissue. The recent development of 2-photon fluorescence lifetime imaging microscopy (2pFLIM) in combination with FRET signaling sensors extensively optimized for 2pFLIM has overcome these problems, allowing the quantification of signaling activity in single synaptic compartments in light scattering brain slices [9, 10*, 11*, 15–17].

2-photon glutamate uncaging to induce plasticity of single spines

Another important technique used to study signaling in single spines is 2-photon glutamate uncaging. It has been demonstrated that photolysis of caged glutamate with 2-photon excitation can excite glutamate receptors on single spines [18]. Furthermore, by uncaging glutamate at a spine in Mg^{2+} free solution, high Ca^{2+} transients through NMDA-type glutamate receptors (NMDARs) are evoked in the stimulated spines [4,19], leading to NMDAR-dependent spine enlargement [5]. It has been further demonstrated that AMPA-type glutamate receptors (AMPA) are recruited in the enlarged synapses, causing LTP in synapse-specific manner [5].

By combining 2-photon glutamate uncaging with 2pFLIM, it is now possible to image signaling while inducing synaptic plasticity in single dendritic spines [9, 10*, 11*]. Using these techniques, the activity of CaMKII and small GTPase proteins HRas, RhoA and Cdc42 was measured in single dendritic spines undergoing structural and functional plasticity [9, 10*, 11*].

CaMKII

CaMKII is one of the most abundant proteins in spines and has been known to play an important role in LTP, experience-dependent cortical plasticity, and many forms of hippocampus-dependent learning and memory [20]. The activity of CaMKII in spines was first imaged with a FRET-based CaMKII sensor Camui-alpha in dissociated neurons. Camui-alpha consists of CaMKII with enhanced cyan fluorescent protein (ECFP) and Venus (a bright variant of yellow fluorescent protein (YFP)) fluorophores tagged to the N- and C-termini, respectively [21]. Later, the sensitivity was much improved by combining 2pFLIM and a modified CaMKII sensor Green Camui-alpha, in which ECFP and Venus are replaced by monomeric enhanced green fluorescent protein(mEGFP) and resonant energy transfer acceptor chromophore (REACH; a non-fluorescent variant of YFP) [10*]. Using this method, CaMKII activation in single spines undergoing structural plasticity and LTP was monitored. CaMKII activity increased in the stimulated spine within ~10 s and decayed with

a time constant of ~10 s. The activation was compartmentalized in the stimulated spines, and did not spread into dendrites.

Small GTPase proteins

Ras superfamily proteins, including the Ras, Rho, Arf and Ran subfamilies, regulate a wide variety of cell functions [22] and many of them are also important for synaptic plasticity [23–25]. These proteins are active when bound to GTP, and inactive when bound to GDP [22]. GTPase activating proteins (GAP) promote the hydrolysis of GTP to GDP, inactivating the GTPase, while guanine nucleotide exchange factors (GEF) promote the switch from GDP to GTP [22]. Active small GTPase proteins bind to effector molecules and activate downstream signals. Thus, by measuring FRET between a small GTPase protein tagged with mEGFP and a small GTPase binding domain of an effector tagged with mRFP or mCherry, one can measure the activity of the small GTPase protein. Using this sensor design, the activation of three proteins, HRas, RhoA and Cdc42, has been measured [9,11].

The activity of HRas, RhoA and Cdc42 increases rapidly in the stimulated spines within ~1 min, and then decays over 3–5 min [9,11]. This transient activity is followed by a sustained activation lasting more than ~30 min for RhoA and Cdc42, but not for HRas. Notably, although these three proteins share similar structure and diffusion constants, their activation profiles are very different (Fig. 1): HRas and RhoA activation diffuses out of stimulated spines, and spreads along their parent dendritic shafts over 5–10 μm , while Cdc42 activation is restricted to the stimulated spines. The gradient of activation at the spine neck is large for Cdc42, much less for RhoA, and almost none for HRas (Fig. 1).

Spine-neck diffusion coupling

The diffusion of proteins from spine to dendrite through the spine neck (spine-neck diffusion coupling) is one of the factors important for determining the spatial profile of proteins [3,4,26]. This parameter has been measured by a technique called fluorescence recovery after photobleaching (FRAP): a neuron is overexpressed with GFP (or its color variant)-tagged molecule and the GFP-molecule in a single spine is bleached [27,28]. The recovery of fluorescence by the movement of the GFP-molecule from the dendrite into the spine indicates the spine-neck coupling time constant. Alternatively, one can photo-activate photo-activatable GFP (paGFP) [29] tagged with a target protein, and measure the decay of paGFP fluorescence [30]. Here, we use the term “FRAP” for both methods as they measure essentially the same parameters.

Diffusion of cytosolic proteins

The spine-neck diffusion time constant (τ_{neck}) of many cytosolic molecules has been measured, being ~100 ms for Ca^{2+} measured with a Ca^{2+} indicator [31] and other synthetic dyes [32], and ~500 ms for GFP variants [9,30]. The time constant τ is considered to be tightly coupled with the geometry of the spine and the diffusion constant of the molecule D . In the simplest model in which spine is a single compartment, τ_{neck} is given by:

$$\tau_{\text{neck}} = G/D \quad (1)$$

where D is the diffusion coefficient, and G is the geometrical factor, which can be given for cytosolic molecule in spherical spine head connected with cylindrical spine neck as:

$$G \sim l_{\text{neck}}^2 V_{\text{head}} / V_{\text{neck}} \quad (2)$$

where V_{head} and V_{neck} are the volume of spine head and neck, respectively, and l_{neck} is the length of the neck [33]. For a typical mushroom spine in hippocampus in adult rats with $V_{\text{head}} \sim 0.25 \mu\text{m}^3$, $l_{\text{neck}} \sim 0.5 \mu\text{m}$ and the neck diameter $d_{\text{neck}} \sim 0.1 \mu\text{m}$ ($V_{\text{neck}} \sim 0.004 \mu\text{m}^3$) [34], G is $\sim 16 \mu\text{m}^2$. For Ca^{2+} indicators and GFP, D in cell is $\sim 100 \mu\text{m}^2/\text{s}$ and $\sim 20 \mu\text{m}^2/\text{s}$ [35], and thus τ can be calculated to be 0.16 and 0.8 s, respectively. These values are similar to the measured values [9,30–32].

It should be noted that τ_{neck} is a weak function of the size of the molecule, because D is proportional to hydrodynamic radius r_h ($D \sim 6\pi\eta r_h$) and thus the cubic root of the mass: even for a molecule with a ~ 100 times larger molecular weight, τ_{neck} is only ~ 5 times larger. Thus, if the molecule can diffuse freely in the cytosol and if the diffusion is purely determined by the spine structure, the spine neck coupling time is less than a few seconds.

Membrane targeted proteins

The membrane targeting of proteins slows down the diffusion efficiently. GFP with a myristoylation domain of MACKS or GAP43 fatty acylation signal domain of GAP43 are ~ 10 times slower than cytosolic GFP (5 – 8 s) [9,36]. Similarly, small GTPase proteins H-Ras, RhoA and Cdc42, which are targeted to the plasma membrane, also show similar time constants at room temperature (3–5 s; Fig. 2) [9,11]. For H-Ras, wildtype protein and a constitutively active mutant (G12V) displayed similar spine-neck coupling (~ 5 s), while Cdc42 and RhoA are slightly less diffusible when they have the constitutively active mutation (~ 5 s) compared to wildtype (~ 3 s). This is presumably because active Cdc42 and RhoA are localized more in the plasma membrane [37]. Spine-neck coupling of synaptic receptors is much slower: $\tau_{\text{neck}} \sim 60\text{--}300$ s for AMPARs [36,38,39*] and ~ 10 min for NMDARs [36].

To formulate the spine-neck time constant of membrane-bound molecule, the volume (V_{head} , and V_{neck}) in Eq. 2 should simply be changed to the surface area (S_{head} and S_{neck}):

$$G \sim l_{\text{neck}}^2 S_{\text{head}} / S_{\text{neck}}. \quad (3)$$

For a mushroom spine with $V_{\text{head}} \sim 0.25 \mu\text{m}^3$, $l_{\text{neck}} \sim 0.5 \mu\text{m}$ and $d_{\text{neck}} \sim 0.1 \mu\text{m}$ [34], S_{head} and S_{neck} are $\sim 1.8 \mu\text{m}^2$ and $\sim 0.16 \mu\text{m}^2$, respectively, and thus $G \sim 3 \mu\text{m}^2$. For H-Ras, D was measured to be $\sim 0.5 \mu\text{m}^2/\text{s}$ at room temperature with single molecule tracking [40,41], and thus τ_{neck} is calculated to be ~ 6 s. This value is consistent with the values measured with FRAP for HRas and other small GTPase proteins (Harvey et al., 2008)[11] (Fig. 2). Interestingly, spine-neck coupling was relatively weak function of the spine volume for small GTPase proteins (Fig. 2).

The diffusion coefficients of AMPARs and NMDARs have been measured to be $\sim 0.01\text{--}0.1 \mu\text{m}^2/\text{s}$ [42–45] and $\sim 0.002\text{--}0.02 \mu\text{m}^2/\text{s}$ [46], and thus τ_{neck} for AMPARs and NMDARs is $\sim 30\text{--}300$ s and $\sim 150\text{--}1500$ s, respectively. These values are again consistent with the measured values [36,38,39*].

“Sticky” molecules

Dendritic spines accumulate high concentration of actin. FRAP experiments revealed that the spine-neck coupling of filamentous actin (F-actin) has two components, ~ 1 min and < 20 min [28]. The rate limiting step for the movement of actin across spine-neck is considered to be treadmilling: an actin monomer (G-actin) binds to the barbed end of a filament, moves toward the pointing end, and diffuses away. Thus, τ_{neck} depends on the length of filament, the speed of the treadmilling and the association/dissociation kinetics of G-actin to F-actin

[28]. The slow component has been found to be tightly integrated F-actin near the bottom of the spine [47].

Proteins in post-synaptic density (PSD) such as PSD-95 can be tightly incorporated into PSD and thus the effective diffusion coefficient is very small. The fast component of spine-neck coupling time constants is $\sim 5 - 100$ min [36,48,49], and the slower component decays over hours [49].

CaMKII interacts with PSD proteins, F-actin, calcium channels, synaptic receptors and so on [50]. Due to these interactions, the effective diffusion constant of CaMKII in spine is expected to be much slower than that in solution ($\sim 20 \mu\text{m}^2/\text{s}$) [10,51]. Indeed, the fast component of the spine-neck coupling time constants of CaMKII was measured to be $\sim 1-3$ min [10,36,52].

Activity-dependent regulation of spine-neck diffusion coupling

Interestingly, the diffusion across the spine neck is subject to activity-dependent plasticity [30,32,53]. For most of spines, τ_{neck} of GFP is ~ 0.5 s [30]. However, it has been reported that there is a small fraction of spines with much longer τ_{neck} (< 5 s) [30]. Furthermore, high neuronal activity can increase the fraction of spines with long τ_{neck} . This spine-neck plasticity can be induced within a few minutes by pairing uncaging with back-propagating action potentials (bAP) [30] or by depolarizing spines to ~ 0 mV [32]. In contrary, Tanaka et al. (2008) found that the spine neck become thicker during spine enlargement induced by 2-photon glutamate uncaging paired with bAPs, thereby probably decreasing τ_{neck} . Notably, this thickening of the spine neck requires protein synthesis [53]. Nonetheless, these studies clearly show that spine-neck diffusion coupling is dynamically regulated by neuronal activity.

Modeling the spatial profile of small GTPase proteins

Having established different molecules with different spatial pattern, we can now model the degree of compartmentalization and verify the model. To create a mathematical model explaining the spatial pattern of small GTPase signaling, we formulated the diffusion of molecules on the plasma membrane in and out of spines [4]. In a stimulated spine, the dynamics of GTPase signaling can be described using the single compartment model:

$$\frac{dC_{\text{head}}(t)}{dt} = -\frac{1}{\tau_{\text{neck}}} (C_{\text{head}}(t) - C_D^0(t)) - \frac{1}{\tau_S} C_{\text{head}}(t) + (1 - C_{\text{head}}(t)) f_{\text{GEF}}(t) \quad (4)$$

where C_{head} and C_D^0 is the fraction of active molecule in the spine and dendrite beneath the spine neck, τ_S is the inactivation time constant in spine, and f_{GEF} is the activity of GEF. Once small GTPase proteins are activated in the stimulated spine and diffuse out of the spine, they diffuse along the dendrite until they are inactivated:

$$\frac{\partial C_D(t, x)}{\partial t} = D \frac{\partial^2 C_D(t, x)}{\partial x^2} - \frac{C_D(t, x)}{\tau_D} \quad (5)$$

where $C_D(t, x)$ is the fraction of active molecule along the dendrite as a function of time t and the distance along the dendrite x , and τ_D is the inactivation time constant in dendrite. The flow of active molecule from the spine to dendrite ($x = 0$) on the plasma membrane can be described as:

$$-2\pi r_D D \frac{\partial C_D(t, x)}{\partial x} \Big|_{x \rightarrow +0} = \frac{S_{head}}{\tau_{neck}} \left(\frac{C_{head}(t) - C_D^0(t)}{2} \right) \quad (6)$$

where r_D is the radius of the dendrite. The steady state solution of Eq. 5–6 is given as:

$$\frac{C_D(x)}{C_{head}} = \alpha_{neck} \exp(-|x|/\lambda), \quad (7)$$

where

$$\alpha_{neck} = \frac{1}{4\pi r_D D^{1/2} \tau_D^{-1/2} \tau_{neck} S_{head}^{-1} + 1} \quad (8)$$

is the gradient of activity at the spine neck, and

$$\lambda = \sqrt{D\tau_D} \quad (9)$$

is the length constant of the decay along the dendrite. While the length constant λ is described only with D and τ_D , the activity gradient at the spine neck α_{neck} includes the structural parameters S_{head} , r_D and τ_{neck} . Interestingly none of these parameters is a function of τ_S (the inactivation time constant in spines).

In the experiments measuring the spatial profile of GTPase proteins, median size of the spine volume before stimulation was 0.23–0.28 μm^3 (0.23, 0.28, 0.28 μm^3 for H-Ras, Cdc42 and RhoA; range 0.05–0.75 μm^3) [9,11], and the volume is enlarged by 3–4 folds in 1–2 min [9,11]. Also, τ_{neck} is relatively constant over a large range of the spine volume (Fig. 2). Thus, we calculated the spatial profile using $S_{head} = 4 \mu\text{m}^2$ ($V_{head} \sim 0.8 \mu\text{m}^3$; after enlargement), $r_D = 0.4 \mu\text{m}$ [4], $D = 0.5 \mu\text{m}^2/\text{s}$ and $\tau_{neck} = 5 \text{ s}$ (Fig. 1, curves). Only one parameter, the inactivation time constant τ_D is obtained by fitting the data as $\tau_D \sim 137 \text{ s}$ for HRas, 44 s for RhoA and 8 s for Cdc42. This simple model fits well to the experimental data (Figure 1b).

When constant τ_{neck} is assumed, the spine enlargement during LTP decreases the signal gradient between spine head and dendrite (Eq. 7, 8). Thus, it is important to measure how τ_{neck} is changed during structural plasticity [30,32,53].

Roles of the signal spreading

2-photon glutamate uncaging allows one to stimulate synapses in a spatially and temporally controlled manner. This technique is thus useful to identify the length scale of many different forms of synaptic plasticity as well as other cellular events. Here we review the hypothetical roles of signals spreading out of spines (Fig. 3).

Spine-specific plasticity

LTP and associated structural plasticity induced by structural plasticity is specific to the stimulated spine [5]. In adjacent spines, neither spine volume nor number of AMPARs changes during these processes [5].

More recently, it has been found that silencing single synapses alters the number of glutamate receptors in the silenced synapses, but not in adjacent synapses [54,55]. Huo et al (2008) [54] inhibited single presynapse by expressing Kir2.1 potassium channels and showed that the number of AMPARs, but not NMDARs, increased in the spines connected to these silenced terminals. The length scale of this form of plasticity is single spine: the number of NMDARs in adjacent, non-silenced spines was unaltered. Lee et al. (2010) [55] silenced presynaptic terminals by expressing tetanus toxin light chain. In contrary to Huo's result, they found that the number of NMDARs containing GluN2B subunit, but not AMPARs, increased in the silenced spine. The NMDARs in adjacent, non-silenced spines was not changed, indicating that this form of plasticity is also spine specific. Further, Ca^{2+} influx through NMDARs increases in the silenced synapse, and this facilitates LTP and associated spine enlargements in the silenced synapses. Although the results are different, both studies show that plasticity induced by silencing synapses can be spine-specific.

Priming of LTP

The spreading signals have been first discovered as priming of LTP in spines adjacent to spines undergoing LTP induction [6]. In this experiment, LTP was induced in a single dendritic spine using 2-photon glutamate uncaging. Then, within 5 minutes after the first stimulation, weak stimulation which usually does not produce plasticity by itself was applied to an adjacent dendritic spine less than $\sim 5 \mu\text{m}$ away from the originally stimulated spine. This subthreshold stimulus was then sufficient to induce LTP. The spatial ($\sim 5 \mu\text{m}$) and temporal (\sim minutes) scale of LTP priming is similar to that of Ras activation. Indeed, the Ras-extracellular signal-regulated kinase (ERK) pathway was found to be required for this facilitation of LTP [9]: to test if the Ras-ERK pathway is required for this form of plasticity, an inhibitor of this pathway (U0126) was applied between the initial LTP-inducing stimulus and the subsequent weak stimulus. LTP in response to the initial LTP-inducing stimulus was not inhibited, but primed LTP in response to the second weak stimulus was inhibited by this manipulation [9]. Furthermore, the second stimulus did not produce any additional Ras activation, suggesting that spreading of Ras is essential to produce the facilitation of plasticity.

Protein synthesis-dependent plasticity

Spine enlargement and LTP induced by glutamate uncaging is not sensitive to protein synthesis inhibitors anisomycin or cyclohexamide. However, protein synthesis-dependent plasticity can be induced in single spines using glutamate uncaging paired with postsynaptic spiking [53]. Alternatively, glutamate uncaging in the presence of brain-derived neurotrophic factor (BDNF) or forskolin (an activator of cAMP signaling) in the bath also can induce protein-synthesis-dependent plasticity [7*,53]. Further, Govindarajan et al. (2011) [7*] found that LTP induced with uncaging and forskolin lasts more than 5 hours (Late LTP or L-LTP) while LTP induced by uncaging alone decays within ~ 3 hours (early-LTP or E-LTP). Once L-LTP is induced in one spine, the E-LTP protocol applied to adjacent spines becomes sufficient to produce L-LTP. The second L-LTP is not sensitive to protein-synthesis inhibitors. Further, the second L-LTP can be induced with a weak stimulation that usually does not produce any spine structural plasticity. This L-LTP facilitation occurs within $\sim 50 \mu\text{m}$ along the dendrite. Thus, the length scale of protein synthesis is an order of magnitude longer than that of Ras activation, E-LTP facilitation or exocytosis events ($\sim 5 \mu\text{m}$). Because the Ras-ERK pathway plays an important role in protein synthesis, factors downstream of Ras-ERK may spread further and cause protein synthesis in the long stretch of the dendrite.

Endosome transport and exocytosis

Insertion of AMPAR in post-synapses is considered to be one of the mechanisms of LTP. Exocytosis of AMPAR containing endosomes is thus a critical step for LTP. Also, exocytosis may provide additional membrane area required for spine enlargement during LTP. It has been reported that only a fraction of spines contain endosomes [56,57], and endosomes are transported into spines during LTP [56] in a Myosin-V dependent mechanism [58]. Thus, there must be signals that diffuse from spines into dendrites to induce the endosome transportation.

More recently, the location of exocytosis of endosomes has been determined using GluA1 subunit tagged with super-ecliptic pHluorin (SEP), a pH-dependent GFP, at its N-terminus [39*, 59–61, 62*]. Because the endosome is acidic, SEP-GluA1 in endosome is quenched. Thus, SEP-GluA1 selectively labels the surface fraction of GluA1. To measure exocytosis, the surface SEP-GluA1 is photo-bleached (while quenched SEP in endosomes is not bleached), and the appearance of bright spots associated with exocytosis is monitored. It has been shown that SEP-GluA1 exocytosis can occur in both spines [59] and dendritic shafts [60,61] during chemical LTP. Also, when LTP is induced in single spines using glutamate uncaging, the rate of exocytosis events is increased for ~ 1 min in adjacent dendrites within ~5 μm from the stimulated spines [39*, 62*] as well as in the stimulated spines [39*], displaying similar pattern with Ras spreading. Further, the activity-dependent increase of exocytosis requires the Ras-ERK pathway, but not CaMKII pathway [39*]. Thus, spreading Ras signaling is indeed important for producing the similar pattern of exocytosis events.

Other potential roles of signal spreading

There are many potential downstream factors of Ras and Rho, which may be activated in the dendritic area adjacent to the stimulated spines (Fig. 3). For example, Ras and Rho signals have been implicated in Ca^{2+} -dependent spine formation [63]. Thus, they may induce the spine formation associated with some forms of LTP [64–66]. Indeed, it has recently been found that newly formed spines tended to appear in close proximity (within a few micrometers) to activated spines during LTP [67]. Also, the dendritic excitability is known to be dependent on ERK [68,69], downstream of Ras, and the length scale of plasticity of dendritic excitability is tens of micrometers [8]. Finally, it is known that late-phase LTP induces gene transcription in the nucleus [70]. When sufficient synapses are activated, signaling molecules may diffuse into nucleus to trigger gene transcription.

Conclusion

Using new optical techniques, we have begun to understand the mechanisms and roles of the spatial regulation of signaling activity in spines and adjacent dendrites. We showed that using a simple mathematical model, the spatial spreading of small GTPase protein could be well described. This model has only a few free parameters, and most of parameters are measurable. Precise measurements of geometrical factors as well as activation/inactivation kinetics of enzymes during the spine structural plasticity will be crucial to predict this spatial spreading more accurately. Further, by comparing the length scale of different signaling pathways and cellular processes, the roles of signal spreading will be clarified.

Acknowledgments

We thank Sridhar Raghavachari for helping mathematical modeling and Nathan Hedrick for critical reading. The work done in Yasuda's lab was supported by NIH and HHMI.

References

1. Augustine GJ, Santamaria F, Tanaka K. Local calcium signaling in neurons. *Neuron*. 2003; 40:331–346. [PubMed: 14556712]
2. Kennedy MB, Beale HC, Carlisle HJ, Washburn LR. Integration of biochemical signalling in spines. *Nat. Rev. Neurosci.* 2005; 6:423–434. [PubMed: 15928715]
3. Sabatini BL, Oertner TG, Svoboda K. The life cycle of Ca(2+) ions in dendritic spines. *Neuron*. 2002; 33:439–452. [PubMed: 11832230]
4. Noguchi J, Matsuzaki M, Ellis-Davies GC, Kasai H. Spine-neck geometry determines NMDA receptor-dependent Ca²⁺ signaling in dendrites. *Neuron*. 2005; 46:609–622. [PubMed: 15944129]
5. Matsuzaki M, Honkura N, Ellis-Davies GC, Kasai H. Structural basis of long-term potentiation in single dendritic spines. *Nature*. 2004; 429:761–766. [PubMed: 15190253]
6. Harvey CD, Svoboda K. Locally dynamic synaptic learning rules in pyramidal neuron dendrites. *Nature*. 2007; 450:1195–1200. [PubMed: 18097401]
7. Govindarajan A, Israely I, Huang SY, Tonegawa S. The dendritic branch is the preferred integrative unit for protein synthesis-dependent LTP. *Neuron*. 2011; 69:132–146. [PubMed: 21220104] Using 2-photon glutamate uncaging, they determined the length scale of protein synthesis-dependent LTP to be not, vert, similarseveral tens micrometers.
8. Losonczy A, Makara JK, Magee JC. Compartmentalized dendritic plasticity and input feature storage in neurons. *Nature*. 2008; 452:436–441. [PubMed: 18368112]
9. Harvey CD, Yasuda R, Zhong H, Svoboda K. The spread of Ras activity triggered by activation of a single dendritic spine. *Science*. 2008; 321:136–140. [PubMed: 18556515]
10. Lee SJ, Escobedo-Lozoya Y, Szatmari EM, Yasuda R. Activation of CaMKII in single dendritic spines during long-term potentiation. *Nature*. 2009; 458:299–304. [PubMed: 19295602] The paper showed a technique to monitor CaMKII activation in single dendritic spines undergoing LTP using 2-photon fluorescence lifetime imaging. CaMKII activation was compartmentalized in stimulated spines. The decay time constant of CaMKII activation was determined to be ~10 s.
11. Murakoshi H, Wang H, Yasuda R. Local, persistent activation of Rho GTPases during plasticity of single dendritic spines. *Nature*. In Press. In this paper, the spatiotemporal dynamics of Rho GTPase proteins RhoA and Cdc42 during structural and functional plasticity of single dendritic spines were measured using 2-photon fluorescence lifetime imaging. Both Cdc42 activation and RhoA activation displayed persistent activation lasting not, vert, similar30 min. Cdc42 activation was compartmentalized in stimulated spines, while RhoA spread into dendrites and adjacent spines.
12. Miyawaki A. Visualization of the spatial and temporal dynamics of intracellular signaling. *Dev. Cell*. 2003; 4:295–305. [PubMed: 12636912]
13. Förster, VT. Intermolecular energy migration and fluorescence (Translation of Förster, T., 1948). In: Mielczarek, EV.; Greenbaum, E.; Knox, RS., editors. *Biological Physics*. American Institute of Physics; 1993. p. 183-221.
14. Lakowicz, JR. *Principles of Fluorescence Spectroscopy*. NY, USA: Plenum; 2006.
15. Yasuda R. Imaging spatiotemporal dynamics of neuronal signaling using fluorescence resonance energy transfer and fluorescence lifetime imaging microscopy. *Curr. Opin. Neurobiol.* 2006; 16:551–561. [PubMed: 16971112]
16. Yasuda R, Harvey CD, Zhong H, Sobczyk A, van Aelst L, Svoboda K. Super-sensitive Ras activation in dendrites and spines revealed by 2-photon fluorescence lifetime imaging. *Nat. Neurosci.* 2006; 9:283–291. [PubMed: 16429133]
17. Murakoshi H, Lee S-J, Yasuda R. Highly sensitive and quantitative FRET-FLIM imaging in single dendritic spines using improved non-radiative YFP. *Brain Cell Biol.* 2008; 36:31–42. [PubMed: 18512154]
18. Matsuzaki M, Ellis-Davies GC, Nemoto T, Miyashita Y, Iino M, Kasai H. Dendritic spine geometry is critical for AMPA receptor expression in hippocampal CA1 pyramidal neurons. *Nat Neurosci.* 2001; 4:1086–1092. [PubMed: 11687814]
19. Sobczyk A, Scheuss V, Svoboda K. NMDA receptor subunit-dependent [Ca²⁺] signaling in individual hippocampal dendritic spines. *J Neurosci.* 2005; 25:6037–6046. [PubMed: 15987933]

20. Lisman J, Schulman H, Cline H. The molecular basis of CaMKII function in synaptic and behavioural memory. *Nat Rev Neurosci.* 2002; 3:175–190. [PubMed: 11994750]
21. Takao K, Okamoto K, Nakagawa T, Neve RL, Nagai T, Miyawaki A, Hashikawa T, Kobayashi S, Hayashi Y. Visualization of synaptic Ca²⁺/calmodulin-dependent protein kinase II activity in living neurons. *J Neurosci.* 2005; 25:3107–3112. [PubMed: 15788767]
22. Takai Y, Sasaki T, Matozaki T. Small GTP-binding proteins. *Physiol Rev.* 2001; 81:153–208. [PubMed: 11152757]
23. Ye X, Carew TJ. Small G protein signaling in neuronal plasticity and memory formation: the specific role of Ras family proteins. *Neuron.* 2010; 68:340–361. [PubMed: 21040840]
24. Tada T, Sheng M. Molecular mechanisms of dendritic spine morphogenesis. *Curr Opin Neurobiol.* 2006; 16:95–101. [PubMed: 16361095]
25. Stornetta RL, Zhu JJ. Ras and Rap Signaling in Synaptic Plasticity and Mental Disorders. *Neuroscientist.* 2010
26. Lee SJ, Yasuda R. Spatiotemporal Regulation of Signaling in and out of Dendritic Spines: CaMKII and Ras. *Open Neurosci J.* 2009; 3:117–127. [PubMed: 20463853]
27. Svoboda K, Tank DW, Denk W. Direct measurement of coupling between dendritic spines and shafts. *Science.* 1996; 272:716–719. [PubMed: 8614831]
28. Star EN, Kwiatkowski DJ, Murthy VN. Rapid turnover of actin in dendritic spines and its regulation by activity. *Nat Neurosci.* 2002; 5:239–246. [PubMed: 11850630]
29. Patterson GH, Lippincott-Schwartz J. A photoactivatable GFP for selective photolabeling of proteins and cells. *Science.* 2002; 297:1873–1877. [PubMed: 12228718]
30. Bloodgood BL, Sabatini BL. Neuronal activity regulates diffusion across the neck of dendritic spines. *Science.* 2005; 310:866–869. [PubMed: 16272125]
31. Sabatini BL, Maravall M, Svoboda K. Ca²⁺ signaling in dendritic spines. *Curr Opin Neurobiol.* 2001; 11:349–356. [PubMed: 11399434]
32. Grunditz A, Holbro N, Tian L, Zuo Y, Oertner TG. Spine Neck Plasticity Controls Postsynaptic Calcium Signals through Electrical Compartmentalization. *J Neurosci.* 2008; 28:13457–13466. [PubMed: 19074019]
33. Byrne MJ, Waxham MN, Kubota Y. The impacts of geometry and binding on CaMKII diffusion and retention in dendritic spines. *J Comput Neurosci.* 2010
34. Harris KM, Jensen FE, Tsao B. Three-dimensional structure of dendritic spines and synapses in rat hippocampus (CA1) at postnatal day 15 and adult ages: implications for the maturation of synaptic physiology and long-term potentiation. *J Neurosci.* 1992; 12:2685–2705. [PubMed: 1613552]
35. Chen Y, Muller JD, Ruan Q, Gratton E. Molecular brightness characterization of EGFP in vivo by fluorescence fluctuation spectroscopy. *Biophys J.* 2002; 82:133–144. [PubMed: 11751302]
36. Sharma K, Fong DK, Craig AM. Postsynaptic protein mobility in dendritic spines: long-term regulation by synaptic NMDA receptor activation. *Mol Cell Neurosci.* 2006; 31:702–712. [PubMed: 16504537]
37. Michaelson D, Silletti J, Murphy G, D'Eustachio P, Rush M, Philips MR. Differential localization of Rho GTPases in live cells: regulation by hypervariable regions and RhoGDI binding. *J Cell Biol.* 2001; 152:111–126. [PubMed: 11149925]
38. Ashby MC, Maier SR, Nishimune A, Henley JM. Lateral diffusion drives constitutive exchange of AMPA receptors at dendritic spines and is regulated by spine morphology. *J Neurosci.* 2006; 26:7046–7055. [PubMed: 16807334]
39. Patterson M, Szatmari EM, Yasuda R. AMPA Receptors are exocytosed in stimulated spines and adjacent dendrites in a Ras-ERK dependent manner during long-term potentiation. *Proc Natl Acad Sci U S A.* 2010; 107:15951–15956. [PubMed: 20733080] This paper was measured showed that AMPAR exocytosis occurs in stimulated spines and adjacent dendrites during LTP. They also showed that the Ras-ERK pathway is required for increasing exocytosis of AMPAR during LTP.
40. Murakoshi H, Iino R, Kobayashi T, Fujiwara T, Ohshima C, Yoshimura A, Kusumi A. Single-molecule imaging analysis of Ras activation in living cells. *Proc Natl Acad Sci U S A.* 2004; 101:7317–7322. [PubMed: 15123831]

41. Lommerse PH, Blab GA, Cognet L, Harms GS, Snaar-Jagalska BE, Spaink HP, Schmidt T. Single-molecule imaging of the H-ras membrane-anchor reveals domains in the cytoplasmic leaflet of the cell membrane. *Biophys J*. 2004; 86:609–616. [PubMed: 14695305]
42. Bats C, Groc L, Choquet D. The interaction between Stargazin and PSD-95 regulates AMPA receptor surface trafficking. *Neuron*. 2007; 53:719–734. [PubMed: 17329211]
43. Giannone G, Hossy E, Levet F, Constals A, Schulze K, Sobolevsky AI, Rosconi MP, Gouaux E, Tampe R, Choquet D, et al. Dynamic superresolution imaging of endogenous proteins on living cells at ultra-high density. *Biophys J*. 2010; 99:1303–1310. [PubMed: 20713016]
44. Heine M, Groc L, Frischknecht R, Beique JC, Lounis B, Rumbaugh G, Hugarir RL, Cognet L, Choquet D. Surface mobility of postsynaptic AMPARs tunes synaptic transmission. *Science*. 2008; 320:201–205. [PubMed: 18403705]
45. Opazo P, Labrecque S, Tigaret CM, Frouin A, Wiseman PW, De Koninck P, Choquet D. CaMKII triggers the diffusional trapping of surface AMPARs through phosphorylation of stargazin. *Neuron*. 2010; 67:239–252. [PubMed: 20670832]
46. Groc L, Heine M, Cognet L, Brickley K, Stephenson FA, Lounis B, Choquet D. Differential activity-dependent regulation of the lateral mobilities of AMPA and NMDA receptors. *Nat Neurosci*. 2004; 7:695–696. [PubMed: 15208630]
47. Honkura N, Matsuzaki M, Noguchi J, Ellis-Davies GC, Kasai H. The subspine organization of actin fibers regulates the structure and plasticity of dendritic spines. *Neuron*. 2008; 57:719–729. [PubMed: 18341992]
48. Sturgill JF, Steiner P, Czervionke BL, Sabatini BL. Distinct domains within PSD-95 mediate synaptic incorporation, stabilization, and activity-dependent trafficking. *J Neurosci*. 2009; 29:12845–12854. [PubMed: 19828799]
49. Gray NW, Weimer RM, Bureau I, Svoboda K. Rapid redistribution of synaptic PSD-95 in the neocortex in vivo. *PLoS Biol*. 2006; 4:e370. [PubMed: 17090216]
50. Merrill MA, Chen Y, Strack S, Hell JW. Activity-driven postsynaptic translocation of CaMKII. *Trends Pharmacol Sci*. 2005; 26:645–653. [PubMed: 16253351]
51. Gaertner TR, Kolodziej SJ, Wang D, Kobayashi R, Koomen JM, Stoops JK, Waxham MN. Comparative analyses of the three-dimensional structures and enzymatic properties of alpha, beta, gamma and delta isoforms of Ca²⁺-calmodulin-dependent protein kinase II. *J Biol Chem*. 2004; 279:12484–12494. [PubMed: 14722083]
52. Okamoto K, Nagai T, Miyawaki A, Hayashi Y. Rapid and persistent modulation of actin dynamics regulates postsynaptic reorganization underlying bidirectional plasticity. *Nat Neurosci*. 2004; 7:1104–1112. [PubMed: 15361876]
53. Tanaka, J-i; Horiike, Y.; Matsuzaki, M.; Miyazaki, T.; Ellis-Davies, GCR.; Kasai, H. Protein Synthesis and Neurotrophin-Dependent Structural Plasticity of Single Dendritic Spines. *Science*. 2008:1152864.
54. Hou Q, Zhang D, Jarzylo L, Hugarir RL, Man HY. Homeostatic regulation of AMPA receptor expression at single hippocampal synapses. *Proc Natl Acad Sci U S A*. 2008; 105:775–780. [PubMed: 18174334]
55. Lee MC, Yasuda R, Ehlers MD. Metaplasticity at single glutamatergic synapses. *Neuron*. 2010; 66:859–870. [PubMed: 20620872]
56. Park M, Penick EC, Edwards JG, Kauer JA, Ehlers MD. Recycling Endosomes Supply AMPA Receptors for LTP. *Science*. 2004; 305:1972–1975. [PubMed: 15448273]
57. Park M, Salgado JM, Ostroff L, Helton TD, Robinson CG, Harris KM, Ehlers MD. Plasticity-Induced Growth of Dendritic Spines by Exocytic Trafficking from Recycling Endosomes. *Neuron*. 2006; 52:817–830. [PubMed: 17145503]
58. Wang Z, Edwards JG, Riley N, Provance DW Jr, Karcher R, Li XD, Davison IG, Ikebe M, Mercer JA, Kauer JA, et al. Myosin Vb mobilizes recycling endosomes and AMPA receptors for postsynaptic plasticity. *Cell*. 2008; 135:535–548. [PubMed: 18984164]
59. Kennedy MJ, Davison IG, Robinson CG, Ehlers MD. Syntaxin-4 defines a domain for activity-dependent exocytosis in dendritic spines. *Cell*. 2010; 141:524–535. [PubMed: 20434989]

60. Yudowski GA, Puthenveedu MA, Leonoudakis D, Panicker S, Thorn KS, Beattie EC, von Zastrow M. Real-Time Imaging of Discrete Exocytic Events Mediating Surface Delivery of AMPA Receptors. *J Neurosci.* 2007; 27:11112–11121. [PubMed: 17928453]
61. Lin D-T, Makino Y, Sharma K, Hayashi T, Neve R, Takamiya K, Huganir RL. Regulation of AMPA receptor extrasynaptic insertion by 4.1N, phosphorylation and palmitoylation. *Nat Neurosci.* 2009; 12:879–887. [PubMed: 19503082]
62. Makino H, Malinow R. AMPA Receptor Incorporation into Synapses during LTP: The Role of Lateral Movement and Exocytosis. *Neuron.* 2009; 64:381–390. [PubMed: 19914186] The authors of this paper measured the spatial pattern of AMPA receptor exocytosis, and showed that the exocytosis events occur in adjacent dendrites during LTP.
63. Saneyoshi T, Fortin DA, Soderling TR. Regulation of spine and synapse formation by activity-dependent intracellular signaling pathways. *Curr Opin Neurobiol.* 2010; 20:108–115. [PubMed: 19896363]
64. Maletic-Savatic M, Malinow R, Svoboda K. Rapid dendritic morphogenesis in CA1 hippocampal dendrites induced by synaptic activity. *Science.* 1999; 283:1923–1927. [PubMed: 10082466]
65. Engert F, Bonhoeffer T. Dendritic spine changes associated with hippocampal long-term synaptic plasticity. *Nature.* 1999; 399:66–70. [PubMed: 10331391]
66. Nagerl UV, Eberhorn N, Cambridge SB, Bonhoeffer T. Bidirectional activity-dependent morphological plasticity in hippocampal neurons. *Neuron.* 2004; 44:759–767. [PubMed: 15572108]
67. De Room M, Klausner P, Muller D. LTP promotes a selective long-term stabilization and clustering of dendritic spines. *PLoS Biol.* 2008; 6:e219. [PubMed: 18788894]
68. Adams JP, Anderson AE, Varga AW, Dineley KT, Cook RG, Pfaffinger PJ, Sweatt JD. The A-type potassium channel Kv4.2 is a substrate for the mitogen-activated protein kinase ERK. *J Neurochem.* 2000; 75:2277–2287. [PubMed: 11080179]
69. Watanabe S, Hoffman DA, Migliore M, Johnston D. Dendritic K⁺ channels contribute to spike-timing dependent long-term potentiation in hippocampal pyramidal neurons. *Proc. Natl. Acad. Sci. USA.* 2002; 99:8366–8371. [PubMed: 12048251]
70. Adams JP, Dudek SM. Late-phase long-term potentiation: getting to the nucleus. *Nat Rev Neurosci.* 2005; 6:737–743. [PubMed: 16136174]

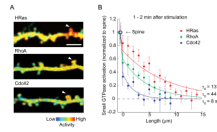


Figure 1. Spatial spreading of small GTPase proteins during structural plasticity

A. The spatial profile of activity of small GTPase proteins HRas, RhoA and Cdc42 imaged with 2-photon fluorescence lifetime imaging microscopy. Bar: 5 μm. Reprinted and modified from [9] and [11].

B. Activation of small GTPase protein normalized to the stimulated spine as a function of the contour distance from the stimulated spines (Dendritic segment at the spine neck = 0).

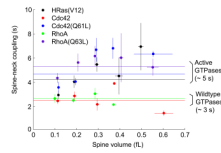


Figure 2. Relationship between spine volume and spine-neck coupling time constants of small GTPase proteins HRas, Cdc42 and RhoA

Spine-neck coupling was measured by photoactivation of paGFP tagged small GTPase proteins. Spine volume was measured from the fluorescence intensity of red fluorescence protein in spines measured with 2-photon microscopy [9, 11]. HRas(V12), Cdc42(Q61L) and RhoA(Q63L) are constitutively active mutants.

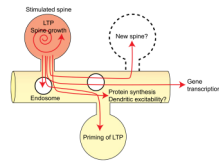


Figure 3. Hypothetical roles of signal spreading